Hindawi
Advances in Mathematical Physics
Volume 2018, Article ID 5370349, 15 pages
https://doi.org/10.1155/2018/5370349

Research Article

Decay Rate and Energy Gap for the Singularity Solution of the Inhomogeneous Landau-Lifshitz Equation on $\mathbb{S}^2$

Penghong Zhong

Department of Mathematics, Guangdong University of Education, Guangzhou 510640, China

Correspondence should be addressed to Penghong Zhong; zhonghong737@163.com

Received 8 March 2018; Revised 1 July 2018; Accepted 9 July 2018; Published 1 August 2018

Academic Editor: Andrei D. Mironov

The singularity solution for the inhomogeneous Landau-Lifshitz (ILL) equation without damping term in n-dimensional space was investigated. The implicit singularity solution was obtained for the case where the target space is on $\mathbb{S}^2$. This solution can be classified into four types that cover the global and local solutions. An estimation of the energy density of one of these types indicates its exact decay rate, which allows a global solution with finite initial energy under $n > 3$. Analysis of the four aperiodic solutions indicates that energy gaps that are first contributions to the literature of ILL will occur for particular coefficient settings, and these are shown graphically.

1. Introduction

The nonlinear ferromagnetic chain model (FCM) has attracted the attention of physicists and mathematicians. For physicists, FCM represents the possibility of describing magnetic field density evolution with various external fields, while mathematicians study the various solutions or excitations in geometrically motive nonlinear models. Quantitative models depicting FCM were proposed by Landau and Lifshitz in 1935 [1], and the Landau-Lifshitz equation (LLE) was proposed to the dynamics of the nonequilibrium magnetism system:

$$S_t = \alpha S \wedge (\triangle S + H) - \beta S \wedge (S \wedge (\triangle S + H)), \quad (\vec{x}, t) \in R^3 \times R, \tag{1}$$

where H is the variational sum of magnetic anisotropy energy and magnetic field energy, $S = (S_1, S_2, S_3)$ denotes magnetization intensity, $\wedge$ is the cross product of Euclidean 3-space R^3, and α and β are constants. If $H = 0$ and $\alpha = 0$, then LLE is the harmonic map heat flow (HMF). Otherwise, when $\beta = 0$, the Gilbert damping vanishes, and when $\beta = 0$ and $H = 0$, the LLE degenerates into the Schrödinger map heat flow (SMF), which is an important equation of differential geometry. SMF can be regarded as a nonlinear Schrödinger equation that contains a derivative term. Although the existence, uniqueness, and the blow-up problem of some nonlinear Schrödinger equations [2–4] are clear, the theorem of SMF becomes more complicated and some further work still needs to be done. Similarly, comparing HMF and some general harmonic system (or even biharmonic equation) [5–8], the mapping system is more complicated than the nonmapping system due to the curvature flow of the Riemannian manifolds.

For clarity, we set J and h as the complex structure and metric on the Kähler manifold, respectively. Different manifolds and their covariant derivatives are M and D, respectively, and we define SMF as

$$\frac{\partial S}{\partial t} = J \sum_{l=1}^{3} D^l \partial_l S. \tag{2}$$

Thus, (2) defines a mapping $S : R^3 \times R \longrightarrow (M, h, J)$, which can degenerate into other subcases; for example, when $M = \mathbb{S}^2$ and $J = S\Lambda$, (2) is the isotropic LLE without Gilbert damping, and if the manifold and complex structure are $\mathscr{H}^2$ and $\dot{\wedge}(\vec{a}\dot{\wedge}\vec{b} = (\vec{a} \wedge \vec{b})\mathrm{diag}\{1, 1, -1\})$, respectively, then (2) is the hyperbolic isotropic LLE without Gilbert damping.

If $M = \mathbb{S}^2$ and $J = S\Lambda$, then (2) can transform into a Schrödinger-type equation using the Hashimoto transform.

Under n dimensional cylindrical coordinates, let $r = |\overrightarrow{x}|$, and the curvature and torsion are, respectively,

$$\kappa = \left(S_r \cdot S_r\right)^{1/2}, \qquad \tau = \frac{S \cdot \left(S_r \Lambda S_{rr}\right)}{\kappa^2}. \tag{3}$$

Then, employing the Hashimoto transform,

$$Q = \frac{\kappa}{2} \exp\left[i \int \tau\left(t, \tilde{r}\right) \mathrm{d}\tilde{r}\right], \tag{4}$$

and (2) transforms to

$$i\frac{\partial}{\partial t}Q + \frac{\partial^2}{\partial r^2}Q + \frac{1}{r}(n-1)\frac{\partial}{\partial r}Q - \frac{1}{r^2}(n-1)Q + 2|Q|^2 Q = 0. \tag{5}$$

If $n = 1$, (5) is the standard cubic Schrödinger equation for which the Lax pair is obtained, and explicit solutions can be constructed using the Bäcklund transformation. Hence, (5) can be regarded as a simple case of (2). Similar to the inhomogeneous Schrödinger equation, (2) (or (1)) can be extended to the inhomogeneous expression. If we add the inhomogeneous term $q(t, \overrightarrow{x})$ to (2), SME can be generalized into the inhomogeneous SME (ILL) proposed by Balakrishnan [9]:

$$\frac{\partial}{\partial t}S = q\left(t, \overrightarrow{x}\right) S \wedge \triangle S + \nabla q\left(t, \overrightarrow{x}\right)\left(S \wedge \nabla S\right), \tag{6}$$

where the inhomogeneous term, $q(t, \overrightarrow{x})$, is a scalar function. Under radially symmetrical coordinates, (6) can be expressed as

$$\frac{\partial}{\partial t}S - q(t,r)\, S \wedge \left(\frac{\partial^2}{\partial r^2}S + \frac{n-1}{r}\frac{\partial}{\partial r}S\right) - \frac{\partial}{\partial r}q(t,r)\left(S \wedge \frac{\partial}{\partial r}S\right) = 0. \tag{7}$$

Using the Hashimoto transform (4), (7) transforms into a nonlinear inhomogeneous Schrödinger equation:

$$i\frac{\partial}{\partial t}Q + q\left(\frac{\partial^2}{\partial r^2}Q + \frac{1}{r}(n-1)\frac{\partial}{\partial r}G - \frac{1}{r^2}(n-1)Q + 2|Q|^2 Q\right) + Q\left(\frac{\mathrm{d}^2}{\mathrm{d}r^2}q + \frac{1}{r}(n-1)\frac{\mathrm{d}}{\mathrm{d}r}q + 2\int\left(\frac{\mathrm{d}}{\mathrm{d}r}q\right)|Q|^2\,\mathrm{d}r + 4(n-1)\int\frac{1}{r}q|Q|^2\,\mathrm{d}r\right) + 2\left(\frac{\mathrm{d}}{\mathrm{d}r}q\right)\frac{\partial}{\partial r}Q = 0. \tag{8}$$

Daniel et al. [10] identified the integrable model (8) by analyzing the singularity structure of its solutions and also discussed Lax pairs, Bäcklund transformation, and soliton-like solutions of (7) (or (8)). They showed that inhomogeneous terms play an important role, and Painlevé analysis indicated that (7) (or (8)) was integrable in arbitrary n dimensions if and only if $q(t,r) = \varepsilon_1 r^{-2(n-1)} + \varepsilon_2 r^{-(n-2)}$.

As all know, the bifurcation structures of the general integrable systems and autonomous differential systems [11–14] are clear due to the properties of Hamiltonian systems [15–18]. However, the structure for the unintegrable system is not so clear. If $q(t,r)$ takes other forms, what would be the solution of (7)? The regularity of the unintegrable case has been somewhat clarified [19, 20] in regard of the singularity behavior of the equation. Two different finite time blowup solutions of (7) were constructed in [20], one being an explicit form and the other being an implicit solution. Careful estimation of the two spatial dimension implicit solutions indicates that the energy density decay rate is $1/r$. However, if the spatial dimension is any integer n, does a global smooth (or blowup) solution of (7) exist? Does (7) also present similar regularity aspects under specific smooth initial data? The regularity of n dimensional ILL remains open.

Many physical phenomena develop singular behavior, for example, boundary layers or blowup solutions. Liu [21] analyzed the concentration set of the stationary weak solutions to LLE for the ferromagnetic spin chain. Based on the Ginzburg-Landau approximation, Wang [22] established the existence of a global weak solution for LLE, $n <= 4$, with respect to smooth initial boundary data, which is smooth from a closed set with locally finite n dimensional parabolic Hausdorff measure. In 2008, Huh [23] constructed infinite energy explicit blowup solutions for the modified LLE. Ding [24] constructed an infinite energy blowup solution for LLE on a hyperbolic target.

The finite energy blowup solution was firstly studied by perturbation methods [25, 26], and it was found that the collapse of a symmetric case with large initial energy formed a singularity where the blowup rate could be estimated by scale invariance. To obtain the required resolution for evolving similar solutions, adaptive mesh refinement (AMR) is required [26–28], which dynamically and locally adds numerical resolution. Although Van Den Berg et al. [26] present a formal analysis and AMR simulation for LLE with the Gilbert term, rigorous proof of blowup for 2-dimensional (2D) LLE remains open. However, Ding et al. [29] proved that $n = 3$ or $n = 4$ dimensional LLE with the Gilbert term will lead to a finite time blowup under specific initial boundary conditions. Some regularity and blowup results for LLE were derived considering the Maxwell field [30, 31].

Although the blowup problem is clear for specific settings (initial state or initial boundary conditions), the blowup problem for ILL is unclear. The one-dimensional ILL will not form a singularity as the inhomogeneous term is periodic [32]. However, if the inhomogeneous term is in some other specific format [33], blowup occurs for the inhomogeneous HMF.

We studied the blowup and energy gap for n dimensional aperiodic ILL on $\mathbb{S}^2$ target and investigated what happens as t tends to infinity when the initial data is smooth and

sufficiently large, in particular whether the solution develops distinct behaviors (finite or global time singularity) under the large data. Global smooth (or blowup) theory for ILL was not established, but we discuss some special solutions that form a singularity in finite time and classify these solutions and analyses based on their energy density.

In Section 2, we obtain a blowup solution for the ILL and derive the exact decay rate of the energy density for that solution. In Section 3, we obtain another local blowup solution that contains an energy gap under the inhomogeneous term and classify this solution into four types. In Section 4, we obtain the decay rate and prove the decreasing (or increasing) property of the local blowup solution for one of these types under some specific coefficient settings. Finally, in Section 5, we summarize the paper and present our conclusions.

2. Blowup Solution on a Sphere

2.1. Blowup Solution Derivation. Selecting the appropriate solution to construct the blowup solution is difficult. Group invariance (under $O(3,1)$ or $SL(2,C)$) can be applied to search for exact solutions of LLE [34–36], but ILL will not admit any group invariance. Following [19, 20, 37], we use cylindrical coordinates,

$$\begin{aligned} S_1(t,r) &= \cos(m(t,r))\sin(f(r)),\\ S_2(t,r) &= \sin(m(t,r))\sin(f(r)),\\ S_3(r) &= \cos(f(r)), \end{aligned} \tag{9}$$

where $r = |\vec{x}|$, $m(t,r)$, and $f(r)$ are functions to be determined.

For simplicity, consider the case where $q(t\vec{x})$ does not contain t and denote $q(r)$, $m(t,r)$, and $f(r)$ as q, m, and f, respectively. Then, from (9), (7) will be greatly simplified and maybe is transformed into

$$\begin{aligned} &2\frac{q\cos(f)\left((\mathrm{d}/\mathrm{d}r)f\right)(\partial/\partial r)m}{\sin(f)} + q\frac{\partial^2}{\partial r^2}m\\ &\quad + \left(\frac{\mathrm{d}}{\mathrm{d}r}q\right)\frac{\partial}{\partial r}m + \frac{(n-1)q(\partial/\partial r)m}{r} = 0 \end{aligned} \tag{10}$$

and

$$\begin{aligned} &q\sin(f)\cos(f)\left(\frac{\partial}{\partial r}m\right)^2 r + \left(\frac{\partial}{\partial t}m\right)\sin(f)r\\ &\quad - q\left(\frac{\mathrm{d}^2}{\mathrm{d}r^2}f\right)r - \left(\frac{\mathrm{d}}{\mathrm{d}r}q\right)\left(\frac{\mathrm{d}}{\mathrm{d}r}f\right)r\\ &\quad - (n-1)q\frac{\mathrm{d}}{\mathrm{d}r}f = 0, \end{aligned} \tag{11}$$

which are nonlinear partial differential equations. To solve these equations, let us assume that m is a variable separation function:

$$m = g(r)h(t) + C, \tag{12}$$

where $g(r)$ and $h(t)$ are dependent on r and t, respectively; and C is a constant. Since $q(t\vec{x})$ does not contain t, $g(r)$ and $h(t)$ are denoted as g and h, respectively. Substituting (12) into (10) and (11),

$$\begin{aligned} &2\left(\frac{\mathrm{d}}{\mathrm{d}r}g\right)q\cos(f)\left(\frac{\mathrm{d}}{\mathrm{d}r}f\right)r\\ &\quad + \left(\frac{\mathrm{d}}{\mathrm{d}r}g\right)\sin(f)\left(\frac{\mathrm{d}}{\mathrm{d}r}q\right)r + q\left(\frac{\mathrm{d}^2}{\mathrm{d}r^2}g\right)\sin(f)r\\ &\quad + (n-1)\left(\frac{\mathrm{d}}{\mathrm{d}r}g\right)q\sin(f) = 0, \end{aligned} \tag{13}$$

$$q\left(\frac{\mathrm{d}^2}{\mathrm{d}r^2}f\right)r + \left(\frac{\mathrm{d}}{\mathrm{d}r}q\right)\left(\frac{\mathrm{d}}{\mathrm{d}r}f\right)r + (n-1)q\frac{\mathrm{d}}{\mathrm{d}r}f = 0, \tag{14}$$

$$\cos(f)\left(\frac{\mathrm{d}}{\mathrm{d}r}g\right)^2 q - g = 0, \tag{15}$$

and

$$h = \frac{1}{t-T}, \tag{16}$$

where $T > 0$.

Solving (13)–(15),

$$f = 2\arctan\left(\mathrm{e}^F\right), \tag{17}$$

$$q = \frac{C_1\left(\mathrm{e}^{-F} + \mathrm{e}^F\right)}{2\left((\mathrm{d}/\mathrm{d}r)F\right)r^{n-1}}, \tag{18}$$

and

$$g = \frac{1}{2}C_3\left(-1 + \mathrm{e}^{-2F}\right)\mathrm{e}^F, \tag{19}$$

where C_1 and C_2 are constants, F is a function of r, and F satisfies

$$\frac{1}{n}r^n - \frac{1}{2}C_3C_1F - \frac{1}{8}C_3C_1\mathrm{e}^{2F} + \frac{1}{8}C_3C_1\mathrm{e}^{-2F} + C_4 = 0, \tag{20}$$

where C_4 is a constant.

The F derivation of (20) is

$$-\frac{1}{4}{C_3}^2C_1\left(\mathrm{e}^{2F} + 2 + \mathrm{e}^{-2F}\right). \tag{21}$$

If C_1 and C_3 are nonzero constants, regardless of the value of F, the left sections of (20) and (21) are continuous functions, and (21) is nonzero. Therefore, according to the implicit function theorem, there exists a function F that satisfies (20), and we have the following conclusion.

Theorem 1. *Assuming that q takes the form of (18) and F satisfies (20), there is a solution of (7):*

$$S_1(t,r) = \frac{2e^F}{1+e^{2F}} \cos\left(\frac{C_3\left(-e^F+e^{-F}\right)}{2(t-T)} + C\right),$$
$$S_2(t,r) = \frac{2e^F}{1+e^{2F}} \sin\left(\frac{C_3\left(-e^F+e^{-F}\right)}{2(t-T)} + C\right), \quad (22)$$
$$S_3(r) = -\frac{-1+e^{2F}}{1+e^{2F}},$$

where C, C_1, C_3, and C_4 are arbitrary constants; and constant $T > 0$.

On $\mathbb{S}^2$, from (9),

$$|S_r|^2 = S_1^2 + S_2^2 + S_3^2 = \left(\frac{d}{dr}f\right)^2 + \sin^2(f)\left(\frac{\partial}{\partial r}m\right)^2, \quad (23)$$

and $((\partial/\partial r)m)^2$ of (23) is

$$\left(\frac{\partial}{\partial r}m\right)^2 = \frac{\left(\cot^2(f)+1\right)^2 \left((d/dr)f\right)^2 {C_2}^2}{(-t+T)^2} = \frac{{C_2}^2 \left((d/dr)F\right)^2 \left(e^{2F}+2+e^{-2F}\right)}{4(-t+T)^2}, \quad (24)$$

which indicates that (22) is a solution of (7) which blows up at T.

The energy density of (22) will also blow up, as can be seen from the energy density:

$$W_E = \frac{C_1 (d/dr) f}{r^{n-1}} + \frac{C_1 \sin^2(f)\left((\partial/\partial r)m\right)^2}{\left((d/dr)f\right) r^{n-1}}. \quad (25)$$

2.2. Decay Rate of the Blowup Solution. From the solutions and the energy density of the upper section, it is difficult to see the decay behavior of energy density. The decay characteristics of the solution determine whether solution energy can be finite value across the whole space. Therefore, we investigate the decay rate of the solution using the implicit solution from Section 2.1.

If we take the derivative of (20) with respect to r,

$$\frac{d}{dr}F = \frac{4r^n}{C_3C_1\left(e^{2F}+2+e^{-2F}\right)}, \quad (26)$$

and, from (17), (24), and (25),

$$W_E = \frac{8e^F}{C_3\left(e^{2F}+2+e^{-2F}\right)\left(1+e^{2F}\right)} + \frac{2C_3\left(e^{3F}+e^{-F}+2e^F\right)}{\left(e^{2F}+2+e^{-2F}\right)\left(1+e^{2F}\right)(-t+T)^2}. \quad (27)$$

From (26), $(d/dr)F|_0 = 0$, so if $r > 0$ and $C_3C_1 > 0$,

$$\frac{d}{dr}F > 0, \quad (28)$$

where, in this case, F is a strictly increasing function in the interval $[0, +\infty)$.

Substituting $F = (n/2)\ln(Kr)$ $(K > 0)$ into the left side of (20),

$$H(r) = \frac{r^n}{n} - \frac{1}{8}C_1C_3(Kr)^n - \frac{1}{4}C_1C_3 n \ln(Kr) + \frac{C_1C_3}{8(Kr)^n} + C_4. \quad (29)$$

If $r \longrightarrow +\infty$ and $(1/8)C_3C_1K^n - 1/n \neq 0$, then, from (20),

$$\lim_{r\longrightarrow+\infty} H(r) = -\text{sign}\left(\frac{1}{8}C_3C_1K^n - \frac{1}{n}\right)\cdot\infty, \quad (30)$$

and if $(1/8)C_3C_1K^n - 1/n = 0$,

$$\lim_{r\longrightarrow+\infty} H(r) = -\frac{n}{4}C_3C_1\cdot\infty = -\infty. \quad (31)$$

Equations (30) and (31) mean that K determines the limit to be a positive or a negative value of $H(r)$. Hence,

$$\frac{n}{2}\ln(K_1r) < F < \frac{n}{2}\ln(K_2r) \quad (0 < K_1 < K_2). \quad (32)$$

Combining $F = (n/2)\ln(Kr)$ and (27),

$$W_E = \frac{8(Kr)^{3/2n}}{C_3\left((Kr)^{2n}+2(Kr)^n+1\right)\left(1+(Kr)^n\right)} + \frac{2C_3\left((Kr)^{5n/2}+2(Kr)^{3n/2}+(Kr)^{n/2}\right)}{\left((Kr)^{2n}+2(Kr)^n+1\right)\left(1+(Kr)^n\right)(-t+T)^2}. \quad (33)$$

From (33), as $r \longrightarrow +\infty$, the decay rate of the energy density is

$$W_E \sim \frac{\widetilde{C}(t)}{r^{n/2}}, \quad (34)$$

where $\widetilde{C}(t)$ is function of t; and as $t \longrightarrow T$, $\overline{C}(t) = \infty$.

Thus, we may obtain the decay rate of the $C_1C_3 > 0$ case. If $C_1C_3 < 0$ and $r \longrightarrow +\infty$, then the decay rate of the energy density can be similarly proven. Therefore,

$$F \longrightarrow -\infty, \quad (35)$$

where F satisfies

$$-\frac{n}{2}\ln(K_1r) > F > -\frac{n}{2}\ln(K_2r), \quad (36)$$

and from (27), if $r \longrightarrow +\infty$, we may estimate the solution

$$W_E \sim \widetilde{C}(t)\,e^F \sim \frac{\widetilde{C}(t)}{r^{n/2}}, \quad (37)$$

where $\widetilde{C}(t)$ is a function of t, where if and only if $t = T$, then $\widetilde{C}(t) = \infty$, which has the limit

$$\lim_{r\longrightarrow+\infty} W_E = 0. \quad (38)$$

Thus, W_E is a continuous function with the limit at $+\infty$ of 0. Hence, whether the energy is a finite value depends on the convergence of W_E at 0. From (20), if $r \longrightarrow 0$,

$$\lim_{r\longrightarrow 0} F = \widehat{C}, \tag{39}$$

where $\widehat{C}$ is constant. Thus,

$$\begin{aligned}\lim_{r\longrightarrow 0} W_E = {} & \frac{8e^{\widehat{C}}}{C_3\left(e^{2\widehat{C}} + 2 + e^{-2\widehat{C}}\right)\left(1 + e^{2\widehat{C}}\right)} \\ & + \frac{2C_3\left(e^{3\widehat{C}} + e^{-\widehat{C}} + 2e^{\widehat{C}}\right)}{\left(e^{2\widehat{C}} + 2 + e^{-2\widehat{C}}\right)\left(1 + e^{2\widehat{C}}\right)(-t+T)^2},\end{aligned} \tag{40}$$

and if $\widehat{C} = 0$, then

$$\lim_{r\longrightarrow 0} W_E = \frac{T^2 - 2tT + t^2 + {C_3}^2}{T^2C_3 - 2TtC_3 + t^2C_3}. \tag{41}$$

We can obtain the initial energy density from (41) by setting $t = 0$:

$$\lim_{r\longrightarrow 0} W_{E_0} = \frac{T^2 + {C_3}^2}{T^2C_3}. \tag{42}$$

From (40), the initial energy density is a finite value and if and only if $t = T$, W_E will be in infinite value. Combining this and the decay behavior as $r \longrightarrow +\infty$, the energy of the finite spatial area can be estimated as

$$\int_0^A q(r)\left|S_r(t,r)\right|^2 r^{n-1}\mathrm{d}r < \overline{C}(t), \tag{43}$$

where A is a constant and $\overline{C}(t) = \infty$ if and only if $t = T$. Furthermore, the total energy of the spatial region is

$$\int_0^\infty q(r)\left|S_r(t,r)\right|^2 r^{n-1}\mathrm{d}r = \infty. \tag{44}$$

From the above analysis, we may conclude that, assuming that q takes the form of (18) and F satisfies (20), there is the following solution of (7).

Theorem 2. *If $C_1C_3 \neq 0$, q takes the form of (18) and F satisfies (20), the energy density of (22) is*

$$W_E \sim \frac{\widetilde{C}(t)}{r^{n/2}}, \tag{45}$$

as

$$r \longrightarrow +\infty, \tag{46}$$

and the energy in $r \in [0, A]$ satisfies

$$E[0,A] = \int_0^A q(r)\left|S_r(t,r)\right|^2 r^{n-1}\mathrm{d}r \le \overline{C}(t), \tag{47}$$

where A is constant; and $\overline{C}(t)$ depends on t, such that as $t \longrightarrow T$, $\overline{C}(t) = \infty$.

Similar to the proof of [20], the decay rate of the norm of gradient can now be estimated. Combining (18) and (26),

$$q = \frac{1}{8}{C_1}^2 r^{-2n+2} e^{-F}\left(1 + e^{2F}\right)C_3\left(e^{2F} + 2 + e^{-2F}\right), \tag{48}$$

and to estimate the decay rate as $r \longrightarrow +\infty$, we substitute $F = (n/2)\ln(Kr)$ $(K > 0)$:

$$\begin{aligned}q = {} & \frac{1}{8}{C_1}^2C_3\left((Kr)^{3n/2} + (Kr)^{-3n/2} + 3(Kr)^{n/2}\right. \\ & \left. + 3(Kr)^{-n/2}\right)r^{-2n+2}.\end{aligned} \tag{49}$$

Hence,

$$q \sim r^{-n/2+2}, \quad r \longrightarrow +\infty. \tag{50}$$

The gradient morn and energy density are related:

$$W_E = q\left|S_r\right|^2, \tag{51}$$

so that, combining Theorem 1 and $q \sim r^{-n/2+2}$, as $r \longrightarrow +\infty$,

$$\left|S_r\right|^2 \sim \frac{\widetilde{C}(t)}{r^2}, \tag{52}$$

where $\widetilde{C}(t)$ is function of t, such that if and only if $t \longrightarrow T$, $\overline{C}(t) = \infty$.

3. Multiple Branches of the Blowup Solutions

We investigate the classification of the blowup solution. Since (7) may contain many solutions different from (22), we extend (22) to a general form to find other solutions. In particular, we use (9) as an undetermined solution and assume that C_i $(i = 1, 2, 3, 4)$, C, and $T > 0$ are constant. We set

$$m = gh + C, \tag{53}$$

where

$$\begin{aligned}g &= C_2 + \frac{1}{2}C_3\left(-1 + e^{-2F}\right)e^F, \\ h &= \frac{1}{t-T},\end{aligned} \tag{54}$$

and

$$q = \frac{C_1\left(e^{-F} + e^F\right)}{2\left((\mathrm{d}/\mathrm{d}r)F\right)r^{n-1}}. \tag{55}$$

Therefore,

$$\frac{\mathrm{d}}{\mathrm{d}r}F = \frac{4r^{n-1}\left(e^{2F}C_3 - 2e^FC_2 - C_3\right)}{C_1{C_3}^2\left(-e^{-2F} + e^{2F} + e^{4F} - 1\right)}. \tag{56}$$

If we set

$$\begin{aligned} C_4 &= \frac{1}{8}C_1C_3\left(e^{2\overline{B}}+e^{-2\overline{B}}\right)+\frac{1}{2}C_1C_2\left(e^{\overline{B}}+e^{-\overline{B}}\right) \\ &\quad+\frac{C_1\overline{B}{C_2}^2}{C_3}+\frac{1}{2}C_1C_3\overline{B} \\ &\quad-\frac{2C_1C_2\sqrt{{C_2}^2+{C_3}^2}}{C_3}\operatorname{arctanh}\left(\frac{e^{\overline{B}}C_3-C_2}{\sqrt{{C_2}^2+{C_3}^2}}\right), \end{aligned} \tag{57}$$

then we can obtain a solution of (56) which satisfies the initial condition $F(0)=\overline{B}$:

$$\begin{aligned} &\frac{1}{n}C_3r^n-\frac{1}{8}{C_3}^2C_1e^{2F}-\frac{1}{2}C_1C_2C_3e^F-\frac{1}{2}{C_3}^2C_1F \\ &\quad+\frac{1}{8}{C_3}^2C_1e^{-2F}-\frac{1}{2}C_3C_1C_2e^{-F}-C_1F{C_2}^2 \\ &\quad+C_3C_4 \\ &\quad+2C_1C_2\sqrt{{C_2}^2+{C_3}^2}\operatorname{arctanh}\left(\frac{e^FC_3-C_2}{\sqrt{{C_2}^2+{C_3}^2}}\right) \\ &=0. \end{aligned} \tag{58}$$

The derivative of the left of (58) is

$$-\frac{1}{4}\frac{{C_3}^3\left(e^{4F}+e^{2F}-e^{-2F}-1\right)C_1}{e^{2F}C_3-2e^FC_2-C_3}. \tag{59}$$

We set C_1, C_2, and $C_3\neq 0$. Thus, (59) is 0 if and only if $F=0$, and

$$F\neq\ln\left(\frac{C_2\pm\sqrt{{C_2}^2+{C_3}^2}}{C_3}\right). \tag{60}$$

Regardless of F value, (59) and the left section of (58) are continuous functions, and (59) is not zero. According to the existence theorem of implicit functions, for any

$$F\in R\setminus\left\{0,\ln\left(\frac{C_2\pm\sqrt{{C_2}^2+{C_3}^2}}{C_3}\right)\right\}, \tag{61}$$

there is an F that satisfies (58).

From the above process, we obtain the following conclusion.

Theorem 3. *Assuming that q takes the form of (18) and F satisfies (58), then there is a solution of (7):*

$$\begin{aligned} &S_1(t,r) \\ &\quad=\frac{2e^F}{1+e^{2F}}\cos\left(\frac{C_3\left(-e^F+e^{-F}\right)}{2(t-T)}+\frac{C_2}{t-T}+C\right), \\ &S_2(t,r) \\ &\quad=\frac{2e^F}{1+e^{2F}}\sin\left(\frac{C_3\left(-e^F+e^{-F}\right)}{2(t-T)}+\frac{C_2}{t-T}+C\right), \\ &S_3(r)=-\frac{-1+e^{2F}}{1+e^{2F}}, \end{aligned} \tag{62}$$

where C, C_1, C_2, C_3, and C_4 are any constants; and $T>0$ is constant.

The energy density of the solution from Theorem 3 is

$$\begin{aligned} &W_E \\ &=\frac{2e^{-F}\left(e^{2F}C_3-2e^FC_2-C_3\right)\left({C_3}^2\left(1+e^{2F}\right)^2+4e^{2F}(t-T)^2\right)}{{C_3}^2\left(1+e^{2F}\right)\left(-e^{-2F}+e^{2F}+e^{4F}-1\right)(-t+T)^2}. \end{aligned} \tag{63}$$

Although (62) is similar to (22), their respective energies ((63) and (27)) are different. In (62), F satisfies (58) which contains arctanh, and this defines the range of F:

$$-1<\frac{e^FC_3-C_2}{\sqrt{{C_2}^2+{C_3}^2}}<1. \tag{64}$$

If

$$\frac{e^FC_3-C_2}{\sqrt{{C_2}^2+{C_3}^2}}=\pm1, \tag{65}$$

then

$$F=\ln\left(\frac{\pm\sqrt{{C_2}^2+{C_3}^2}+C_2}{C_3}\right). \tag{66}$$

For (56), if F takes the form of (66), the right of (56) is 0, and F_r is 0.

We must solve

$$\frac{C_3e^{2F}-2C_2e^F-C_3}{\left(-e^{-2F}+e^{2F}+e^{4F}-1\right)C_1}>0, \tag{67}$$

which can be expressed as

$$\frac{C_3}{C_1}\frac{\left(e^F-\left(C_2+\sqrt{{C_2}^2+{C_3}^2}\right)/C_3\right)\left(e^F-\left(C_2-\sqrt{{C_2}^2+{C_3}^2}\right)/C_3\right)}{\left(e^{4F}-1\right)\left(e^{-2F}+1\right)}>0. \tag{68}$$

Table 1: Evolution of F where $C_3 > 0$ and $r > 0$.

	$C_3 > 0,\ C_2 > 0$	$C_3 > 0,\ C_2 < 0$
$C_1 > 0$	If $0 < F < \ln\left(\frac{\sqrt{{C_2}^2 + {C_3}^2} + C_2}{C_3}\right)$, $F_r < 0$ If $-\infty < F < 0$, $F_r > 0$	If $-\infty < F < \ln\left(\frac{\sqrt{{C_2}^2 + {C_3}^2} + C_2}{C_3}\right)$, $F_r > 0$
$C_1 < 0$	If $0 < F < \ln\left(\frac{\sqrt{{C_2}^2 + {C_3}^2} + C_2}{C_3}\right)$, $F_r > 0$ If $-\infty < F < 0$, $F_r < 0$	If $-\infty < F < \ln\left(\frac{\sqrt{{C_2}^2 + {C_3}^2} + C_2}{C_3}\right)$, $F_r < 0$

Table 2: Evolution of F with $C_3 < 0$ and $r > 0$.

	$C_3 < 0, C_2 < 0$	$C_3 < 0, C_2 > 0$
$C_1 > 0$	If $0 < F < \ln\left(\frac{-\sqrt{{C_2}^2 + {C_3}^2} + C_2}{C_3}\right)$, $F_r < 0$ If $-\infty < F < 0$, $F_r > 0$	If $-\infty < F < \ln\left(\frac{-\sqrt{{C_2}^2 + {C_3}^2} + C_2}{C_3}\right)$, $F_r < 0$
$C_1 < 0$	If $0 < F < \ln\left(\frac{-\sqrt{{C_2}^2 + {C_3}^2} + C_2}{C_3}\right)$, $F_r > 0$ If $-\infty < F < 0$, $F_r < 0$	If $-\infty < F < \ln\left(\frac{-\sqrt{{C_2}^2 + {C_3}^2} + C_2}{C_3}\right)$, $F_r > 0$

If $C_3 > 0$,

$$\frac{\sqrt{{C_2}^2 + {C_3}^2} + C_2}{C_3} > 0, \tag{69}$$

and

$$\frac{-\sqrt{{C_2}^2 + {C_3}^2} + C_2}{C_3} < 0. \tag{70}$$

Solving

$$\left(e^{4F} - 1\right)\left(e^{-2F} + 1\right) > 0, \tag{71}$$

we obtain

$$F > 0. \tag{72}$$

Similarly, solving

$$\left(e^{4F} - 1\right)\left(e^{-2F} + 1\right) < 0, \tag{73}$$

we obtain

$$F < 0. \tag{74}$$

If $C_3 > 0$ and $C_2 > 0$, then the inequality is

$$\ln\left(\frac{\sqrt{{C_2}^2 + {C_3}^2} + C_2}{C_3}\right) > 0, \tag{75}$$

and if $C_3 > 0$ and $C_2 < 0$, then

$$\ln\left(\frac{\sqrt{{C_2}^2 + {C_3}^2} + C_2}{C_3}\right) < 0. \tag{76}$$

Thus, if $C_3 > 0$, $C_2 > 0$, $C_1 < 0$, and

$$0 < F < \ln\left(\frac{\sqrt{{C_2}^2 + {C_3}^2} + C_2}{C_3}\right), \tag{77}$$

then (68) holds, and since $r > 0$,

$$F_r > 0. \tag{78}$$

If $r > 0$, $C_3 > 0$, $C_2 < 0$, $C_1 > 0$, and

$$-\infty < F < \ln\left(\frac{\sqrt{{C_2}^2 + {C_3}^2} + C_2}{C_3}\right), \tag{79}$$

then

$$F_r > 0. \tag{80}$$

Similarly, if $C_3 < 0$, we can solve F from $F_r > 0$, and we can solve $F_r < 0$ for the $C_3 > 0$ (or $C_3 < 0$) case. From (58) and (56), if $C_3 > 0$, the change of F_r is shown in Table 1.

Similar to Table 1, if $C_3 < 0$, the change of F_r is shown in Table 2.

From Tables 1 and 2, F satisfying (58) can be subdivided into the following categories:

(1) $C_3 > 0$, $C_2 > 0$ and $C_1 > 0$ (or $C_3 < 0$, $C_2 < 0$ and $C_1 > 0$).

F is a continuous curve. If $F = 0$, solving (58),

$$r_0 = \left[\frac{n}{C_3} \left(2 \operatorname{arctanh} \left(\frac{-C_3 + C_2}{\sqrt{{C_2}^2 + {C_3}^2}} \right) \cdot \sqrt{{C_2}^2 + {C_3}^2} C_1 C_2 + C_1 C_2 C_3 - C_3 C_4 \right) \right]^{1/n}, \tag{81}$$

and (56) can be expressed as

$$r^{n-1} \frac{\mathrm{d}r}{\mathrm{d}F} = \frac{C_1 {C_3}^2 \left(-\mathrm{e}^{-2F} + \mathrm{e}^{2F} + \mathrm{e}^{4F} - 1 \right)}{4 \left(\mathrm{e}^{2F} C_3 - 2\mathrm{e}^{F} C_2 - C_3 \right)}. \tag{82}$$

If the right section of (82) is 0, then $F = 0$. Hence, $r_F = 0$ as $r = r_0$. Thus, the tangent of F is perpendicular to the $r-$ axis at $(r_0, 0)$.

If $r = 0$, then $F_r = 0$ from (56). Hence, the tangent of F is parallel to the $r-$axis at $(0, F(0))$. Specifically, in the fourth quadrant of the rF coordinate system, F is monotonically increasing and $r \in [0, r_0]$. In the first quadrant, F is monotonically decreasing and $r \in [0, r_0]$.

For example, if $n = 2$, $C_1 = C_2 = C_3 = 1$, and $C_4 = 0$, then (58) is

$$\frac{1}{2} r^2 - \frac{1}{8} \mathrm{e}^{2F} - \frac{1}{2} \mathrm{e}^{F} - \frac{3}{2} F - \frac{1}{2} \mathrm{e}^{-F} + \frac{1}{8} \mathrm{e}^{-2F} + 2\sqrt{2} \operatorname{arctanh} \left(\frac{1}{2} \mathrm{e}^{F} \sqrt{2} - \frac{1}{2} \sqrt{2} \right) = 0, \tag{83}$$

and the evolution of F, determined by (83), is shown in Figure 1.

(2) $C_3 > 0$, $C_2 > 0$ and $C_1 < 0$ (or $C_3 < 0$, $C_2 < 0$ and $C_1 < 0$).

The evolution of F in the first and the fourth quadrant are opposite that of case (1). In the fourth quadrant, F is monotonically decreasing, and in the first quadrant, F is monotonically increasing. The tangent of F is perpendicular to the $F-$axis at $(0, F(0))$. If we set

$$F_{\max} = \max \left(\ln \left(\frac{\sqrt{{C_2}^2 + {C_3}^2} + C_2}{C_3} \right), \ln \left(\frac{-\sqrt{{C_2}^2 + {C_3}^2} + C_2}{C_3} \right) \right), \tag{84}$$

the maximum value of F in first quadrant will not exceed $F_{\max}$.

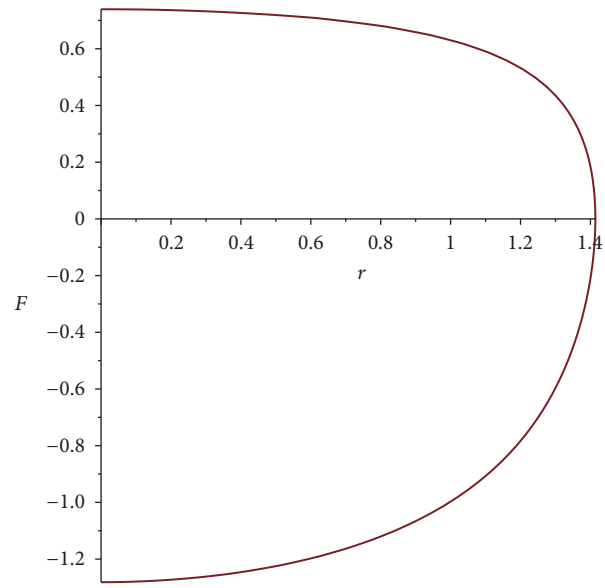

Figure 1: Evolution of F from (83) with $r \in [0, 2]$ and $F \in [-3, 3]$.

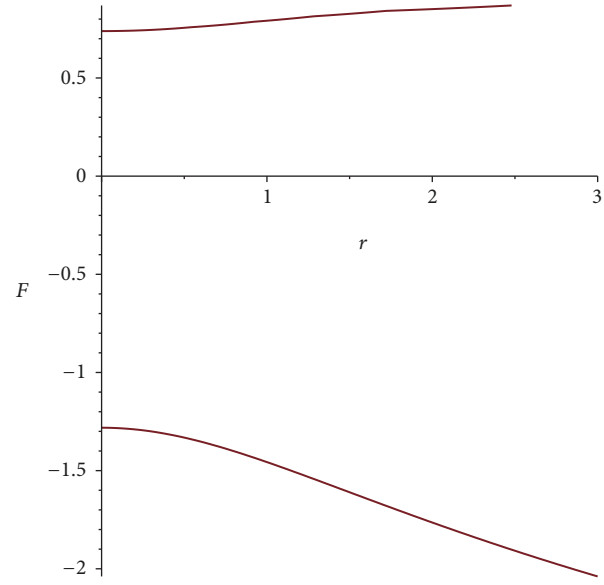

Figure 2: Evolution of F from (85) with $r \in [0, 3]$ and $F \in [-3, 2.5]$.

Specifically, if $n = 2$, $C_1 = -1$, $C_2 = C_3 = 1$, and $C_4 = 0$, then (58) is

$$\frac{1}{2} r^2 + \frac{1}{8} \mathrm{e}^{2F} + \frac{1}{2} \mathrm{e}^{F} + \frac{3}{2} F + \frac{1}{2} \mathrm{e}^{-F} - \frac{1}{8} \mathrm{e}^{-2F} + 2\sqrt{2} \operatorname{arctanh} \left(-\frac{1}{2} \mathrm{e}^{F} \sqrt{2} + \frac{1}{2} \sqrt{2} \right) = 0, \tag{85}$$

and the evolution of F from (85) is shown in Figure 2.

(3) $C_3 > 0$, $C_2 < 0$ and $C_1 > 0$ (or $C_3 < 0$, $C_2 > 0$ and $C_1 < 0$).

F is completely in the fourth quadrant, and is monotonically increasing. The maximum value of F will not

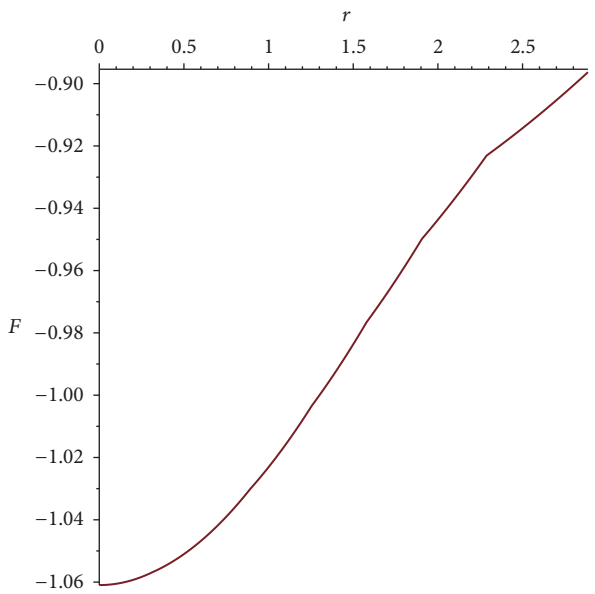

FIGURE 3: Evolution of F from (86) with $r \in [0, 5]$ and $F \in [-4, 4]$.

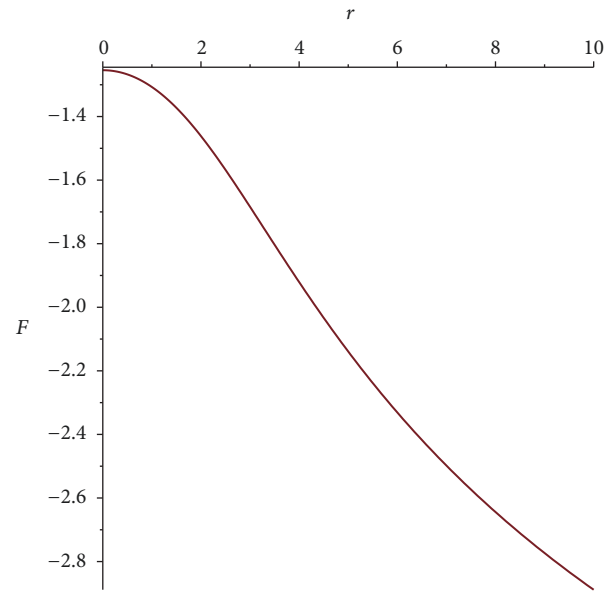

FIGURE 4: Evolution of F from (87) with $r \in [0, 10]$ and $F \in [-4, 4]$.

exceed $F_{\max}$, and the curve in this quadrant has lower bound $F(0)$.

For example, when $n = 2$, $C_1 = 1$, $C_2 = -1$, $C_3 = 1$, and $C_4 = 1$, (58) is

$$\frac{1}{2}r^2 - \frac{1}{8}e^{2F} + \frac{1}{2}e^{F} - \frac{3}{2}F + \frac{1}{2}e^{-F} + \frac{1}{8}e^{-2F} + 1 + 2\sqrt{2}\,\operatorname{arctanh}\left(-\frac{1}{2}e^{F}\sqrt{2} - \frac{1}{2}\sqrt{2}\right) = 0, \tag{86}$$

and Figure 3 shows the evolution of F from (86) with $r \in [0, 5]$ and $F \in [-4, 4]$.

(4) $C_3 > 0$, $C_2 < 0$ and $C_1 < 0$ (or $C_3 < 0$, $C_2 > 0$ and $C_1 > 0$).

F is monotonically decreasing in the fourth quadrant, with upper bound $F(0)$.

Cases (1) and (2) are multi-value, i.e., for each r, There are two values of F. We call these multi-branch functions. However, there is only a single monotonic function for cases (3) and (4).

Let us select some specific parameters and investigate the characteristic solutions. If $n = 2$, $C_1 = C_2 = -1$, $C_3 = 1$, and $C_4 = 1$, then (58) is

$$\frac{1}{2}r^2 + \frac{1}{8}e^{2F} - \frac{1}{2}e^{F} + \frac{3}{2}F - \frac{1}{2}e^{-F} - \frac{1}{8}e^{-2F} + 1 - 2\sqrt{2}\,\operatorname{arctanh}\left(-\frac{1}{2}e^{F}\sqrt{2} - \frac{1}{2}\sqrt{2}\right) = 0, \tag{87}$$

and the evolution of (87) is shown in Figure 4.

In (56), we may regard F as a function of r and z and decompose (56) as

$$\frac{d}{dz}F = 4r^{n-1}\left(e^{2F}C_3 - 2e^{F}C_2 - C_3\right), \tag{88}$$

and

$$\frac{d}{dz}r = C_1{C_3}^2\left(-e^{-2F} + e^{2F} + e^{4F} - 1\right). \tag{89}$$

$F(z)$ and $r(z)$ cannot be expressed as a Hamiltonian system; that is, there is no function $H(F, r)$ such that

$$\frac{\partial}{\partial F}H(F, r) = \frac{d}{dz}r, \qquad \frac{\partial}{\partial r}H(F, r) = \frac{d}{dz}F. \tag{90}$$

Therefore, (90) are noncompatible systems. Solving the first equation of (90),

$$H(F, r) = -C_1{C_3}^2\left(-\frac{1}{2}e^{-2F} - \frac{1}{2}e^{2F} - \frac{1}{4}e^{4F}\right) - C_1{C_3}^2F + F_1(r), \tag{91}$$

where F_1 is a function that is only dependent on r; and solving the second equation of (90),

$$H(F, r) = -\frac{4r^n\left(2e^{F}C_2 - e^{2F}C_3 + C_3\right)}{n} + F_2(F), \tag{92}$$

where F_2 is a function that is only dependent on F.

Since (91) and (92) are contradictory expressions, (90) is an incompatible system.

Equations (88)-(89) contain more solutions than (58). The evolution of these equations can also be classified into four types as follows:

1. Multibranch elliptic case I: $C_3 > 0$, $C_2 > 0$, and $C_1 > 0$ (or $C_3 < 0$, $C_2 < 0$, and $C_1 > 0$).
2. Multibranch hyperbolic case I: $C_3 > 0$, $C_2 > 0$, and $C_1 < 0$ (or $C_3 < 0$, $C_2 < 0$, and $C_1 < 0$).

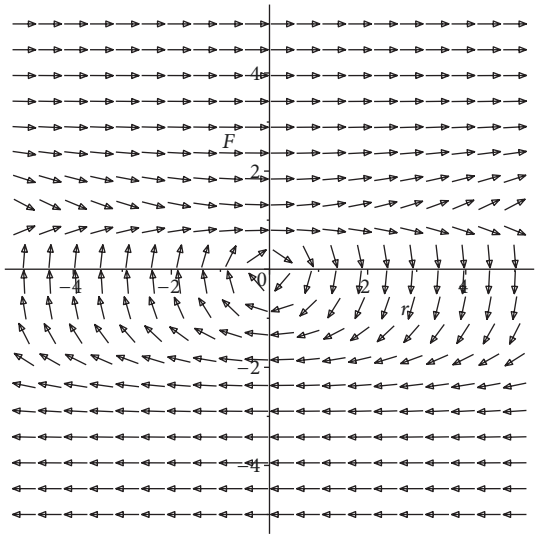

Figure 5: Multibranch elliptic case I: evolution of F ($C_1 = C_2 = C_3 = 1$).

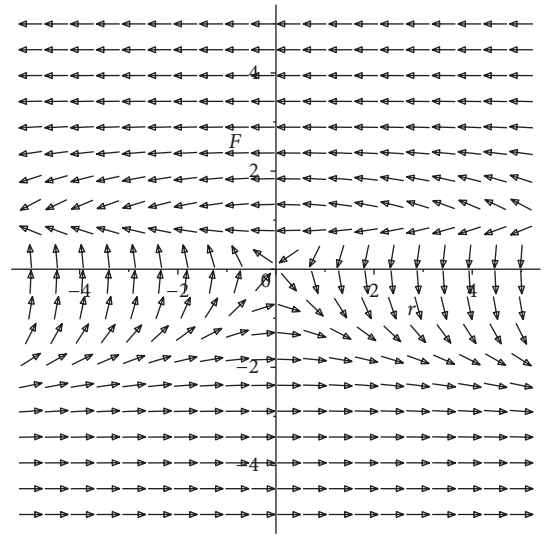

Figure 6: Multibranch hyperbolic case I: distribution of F ($C_1 = -1$ and $C_2 = C_3 = 1$).

3. Multibranch hyperbolic case II: $C_3 > 0$, $C_2 < 0$, and $C_1 > 0$ (or $C_3 < 0$, $C_2 > 0$, and $C_1 < 0$).
4. Multibranch elliptic case II: $C_3 > 0$, $C_2 < 0$, and $C_1 < 0$ (or $C_3 < 0$, $C_2 > 0$, and $C_1 > 0$).

To see the evolution of these four solutions directly, we set $n = 2$ and C_1, C_2, and C_3 as follows:

1. $C_1 = C_2 = C_3 = 1$.
2. $C_1 = -1$ and $C_2 = C_3 = 1$.
3. $C_1 = 1$, $C_2 = -1$, and $C_3 = 1$.
4. $C_1 = C_2 = -1$ and $C_3 = 1$.

Figures 5–8 show the orientation fields for these four cases in the rF coordinate, respectively.

The direction of vector field in Figure 5 is opposite to that of Figure 8, and the direction of Figure 6 is opposite to that of Figure 7. Figures 5 and 8 (or Figures 6 and 7) are very similar. However, in Section 4, we show that the energy densities suggest that all of these four multibranch cases are distinct.

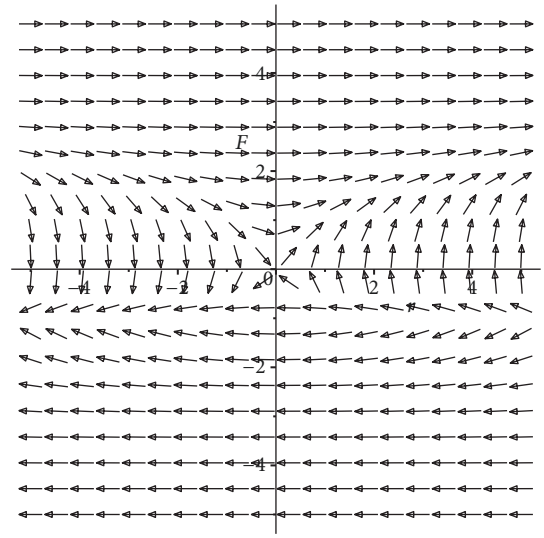

Figure 7: Multibranch hyperbolic case II: evolution of F ($C_1 = 1$, $C_2 = -1$, and $C_3 = 1$).

4. Blowup Solution and Energy Gap

The solutions presented in Sections 2 and 3 will blow up in finite time, but the energy of the solution presented in Section 2 is infinite on all spatial regions. However, can (7) (or (6)) contain some finite energy solutions on the sphere, since solution (62) presented in Section 3 contains some finite energy subcases? In this section, we investigate the blowup solution (62) and particularly the finite energy subcases.

Let us analyze the properties of the energy density (63) of solution (62). Since (63) contains more parameters than (27), the evolution of F_r is more complex for (56) than (26), which leads to more complex evolutionary behavior of (63).

If $C_3 > 0$, $C_2 < 0$, and $C_1 < 0$ (or $C_3 < 0$, $C_2 > 0$, and $C_1 > 0$), then F_r is negative in $[0, +\infty)$, as shown in Figures 4 and 8. Substituting $F = -(n/2)\ln(Lr)$ $(L > 0)$ into the left of (58), we obtain a function $J(r)$, with the limit

$$\lim_{r \longrightarrow +\infty} J(r) = \frac{1}{8n} C_3 \operatorname{sign}\left(L^n n C_1 C_3 + 8\right)) \cdot \infty, \tag{93}$$

where $K^n n C_1 C_3 + 8 \neq 0$.

From (93), the positive and negative of $\lim_{r \longrightarrow +\infty} J(r)$ can be determined by L; that is,

$$-\frac{n}{2}\ln\left(L_1 r\right) > F > -\frac{n}{2}\ln\left(L_2 r\right) \quad \left(0 < L_1 < L_2\right),\ r \longrightarrow +\infty. \tag{94}$$

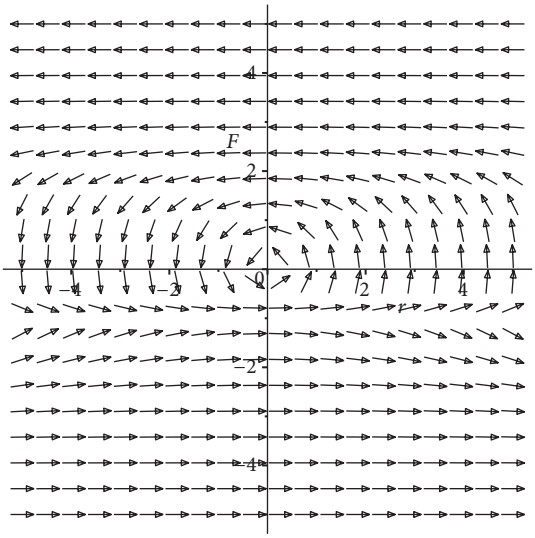

FIGURE 8: Multibranch elliptic case II: distribution of F ($C_1 = C_2 = -1$ and $C_3 = 1$).

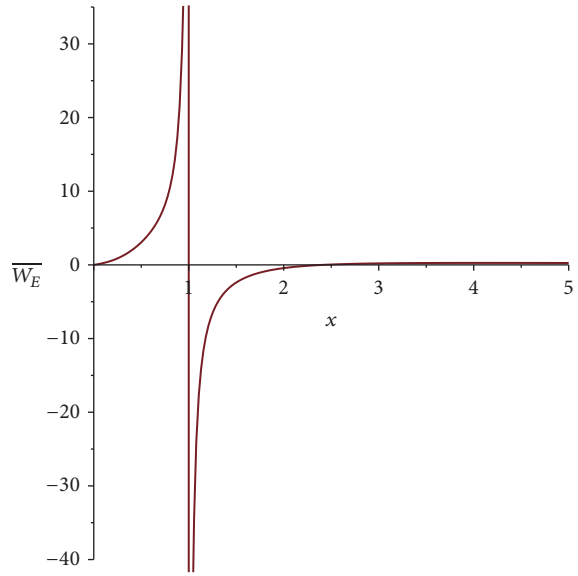

FIGURE 9: Relationship of $\overline{W}_E$ and x with $C_1 = C_2 = C_3 = C_5 = 1$.

Substituting $F = -(n/2)\ln(Lr)$ into (63), the decay rate of the energy density as $r \longrightarrow +\infty$ is

$$W_E \sim \frac{\widetilde{C}(t)}{r^{n/2}}, \tag{95}$$

where $\widetilde{C}(t)$ is a function of t, such that as $t \longrightarrow T$, $\overline{C}(t) = \infty$.

Similar to the proof of Theorem 2, we have the following corollary.

Corollary 4. *If F satisfies (58), $C_3 > 0$, $C_2 < 0$, and $C_1 < 0$ (or $C_3 < 0$, $C_2 > 0$, and $C_1 > 0$), then $r \longrightarrow +\infty$; the energy density of (62) is*

$$W_E \sim \frac{\widetilde{C}(t)}{r^{n/2}}, \tag{96}$$

and the energy in $r \in [0, A]$ satisfies

$$E[0, A] = \int_0^A q(r) \left|S_r(t, r)\right|^2 r^{n-1} \mathrm{d}r \le \overline{C}(t), \tag{97}$$

where A is constant; and $\overline{C}(t)$ is only dependent on t, such that as $t \longrightarrow T$, $\overline{C}(t) = \infty$.

In Corollary 4, parameters C_3, C_2, and C_1 belong to one type from Table 1 (or Table 2). The other three parameters types were divided into two types: $C_3C_2 > 0$ and $C_3C_2 < 0$.

If $t - T = C_5$, then (63) may be expressed as

$$\overline{W}_E = \frac{2\left(\mathrm{e}^{2F}C_3 - 2\mathrm{e}^{F}C_2 - C_3\right)\left(C_3{}^2\left(1 + \mathrm{e}^{2F}\right)^2 + 4\mathrm{e}^{2F}C_5{}^2\right)}{C_5{}^2\mathrm{e}^{F}\left(1 + \mathrm{e}^{2F}\right)\left(-\mathrm{e}^{-2F} + \mathrm{e}^{2F} + \mathrm{e}^{4F} - 1\right)}, \tag{98}$$

and the monotonicity of (63) and that of (98) are the same under $t - T = C_5$. Substituting $F = \ln(x)$ into (98),

$$\overline{W}_E = \frac{2\left(x^2C_3 - 2xC_2 - C_3\right)\left(C_3{}^2x^4 + 2C_3{}^2x^2 + 4x^2C_5{}^2 + C_3{}^2\right)x}{C_5{}^2\left(x^2 + 1\right)\left(x^6 + x^4 - x^2 - 1\right)}. \tag{99}$$

Let us separate one equation from this, such as

$$x^2C_3 - 2xC_2 - C_3 = 0, \tag{100}$$

and solve to obtain

$$x_{1,2} = \frac{\pm\sqrt{C_2{}^2 + C_3{}^2} + C_2}{C_3}. \tag{101}$$

Thus, if $x = C_2/C_3$, the left section of (100) achieves its maximum or minimum value.

The derivative of the left of (99) is

$$\begin{aligned}\left(\overline{W}_E\right)_x = {} & -2C_5{}^{-2}\left(x^6 + x^4 - x^2 - 1\right)^{-2}\left(x^{10}C_3{}^3\right. \\ & - 4x^9C_2C_3{}^2 - x^8C_3{}^3 + 12x^8C_3C_5{}^2 - 8x^7C_2C_3{}^2 \\ & - 32x^7C_2C_5{}^2 - 2x^6C_3{}^3 - 36x^6C_3C_5{}^2 \\ & - 8x^5C_2C_3{}^2 + 32x^5C_2C_5{}^2 + 2x^4C_3{}^3 \\ & + 36x^4C_3C_5{}^2 - 8x^3C_2C_3{}^2 - 32x^3C_2C_5{}^2 + x^2C_3{}^3 \\ & \left. - 12x^2C_3C_5{}^2 - 4xC_2C_3{}^2 - C_3{}^3\right).\end{aligned} \tag{102}$$

If $C_1 = C_2 = C_3 = C_5 = 1$, then the exact relationship of $\overline{w}_E$ and x (or $\overline{w}_E$ and F) is shown in Figure 9 (Figure 10).

Figure 11 shows the evolution of energy density from (63) for multi ranch elliptic case I with $C_1 = C_2 = C_3 = 1$

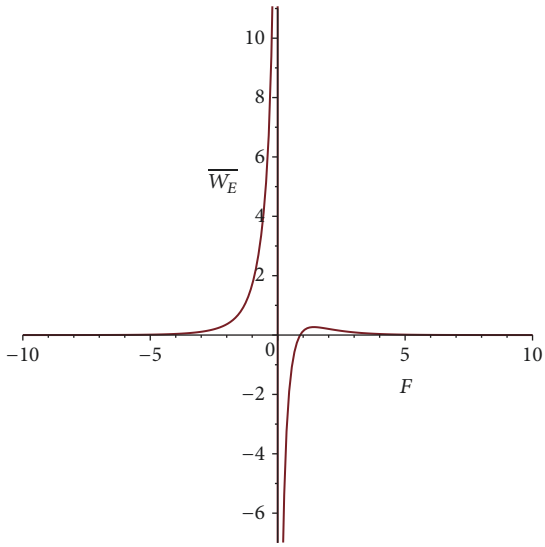

Figure 10: Relationship of $\overline{W}_E$ and F with $C_1 = C_2 = C_3 = C_5 = 1$.

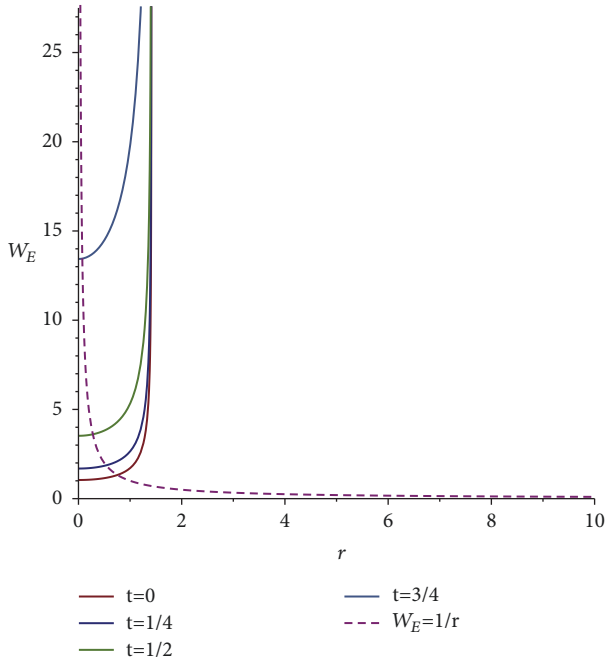

Figure 11: W_E at different times with $C_1 = C_2 = C_3 = 1$ and $C_4 = 0$.

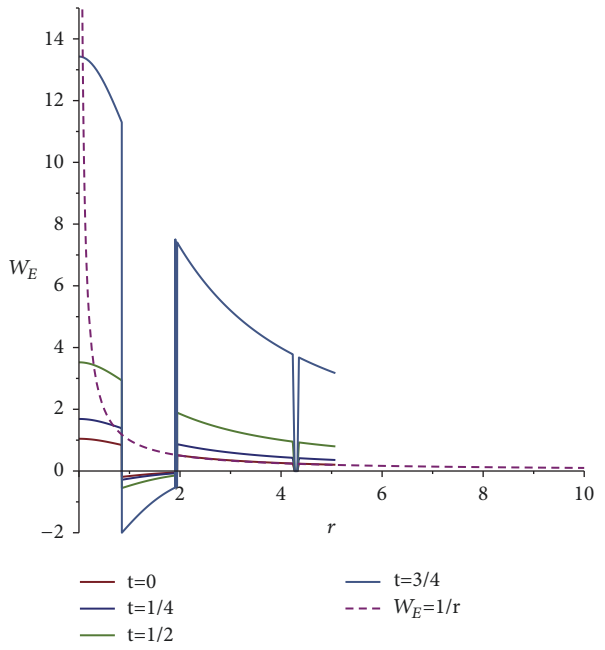

Figure 12: W_E in different time under $C_1 = -1$, $C_2 = C_3 = 1$, and $C_4 = 0$.

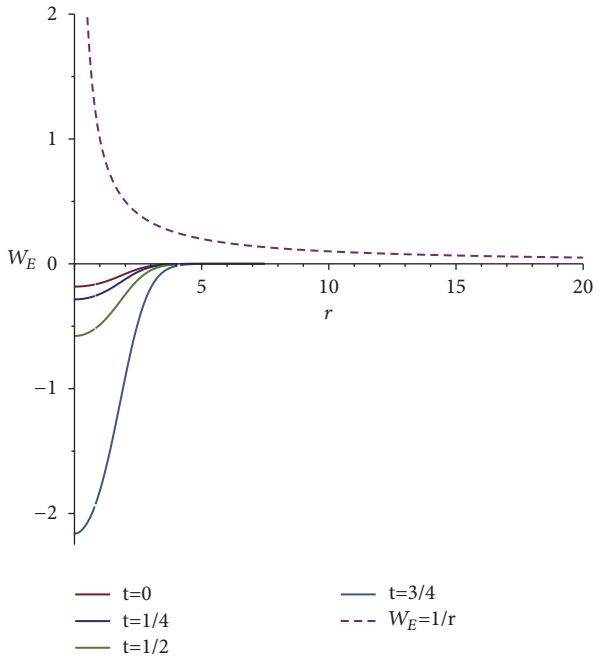

Figure 13: W_E for different times with $C_1 = C_3 = -1$ and $C_2 = C_4 = 1$.

and $C_4 = 0$, and Figure 12 shows multibranch hyperbolic case I with $C_1 = -1$, $C_2 = C_3 = 1$, and $C_4 = 0$. In these two cases, $n = 2$ and $T = 1$. The behavior is shown for $t = 0, 1/4, 1/2, 3/4$, and the function $W_E = 1/r$.

The multibranch elliptic case I (Figure 11) is a local solution that terminates at some point of r. The multibranch hyperbolic case I (Figure 12) is also a local solution. However, there are some energy gaps on W_E. Figure 13 shows the evolution of multibranch hyperbolic case II with $C_1 = C_3 = -1$ and $C_2 = C_4 = 1$ is also local with some energy gaps.

The situation for the multibranch elliptic case II is different from the other three cases. As predicted in Corollary 4, this solution diverges, as shown in Figure 14 with $C_1 = C_2 = -1$ and $C_3 = C_4 = 1$. W_E is a global solution and is close to zero as $r \longrightarrow \infty$. Near the W_E peaks, there are also some energy gaps.

We present some connections of ILL with real physics in the ending of this section. Clearly, we return the continuous ILL model back to the discrete Heisenberg model in the real

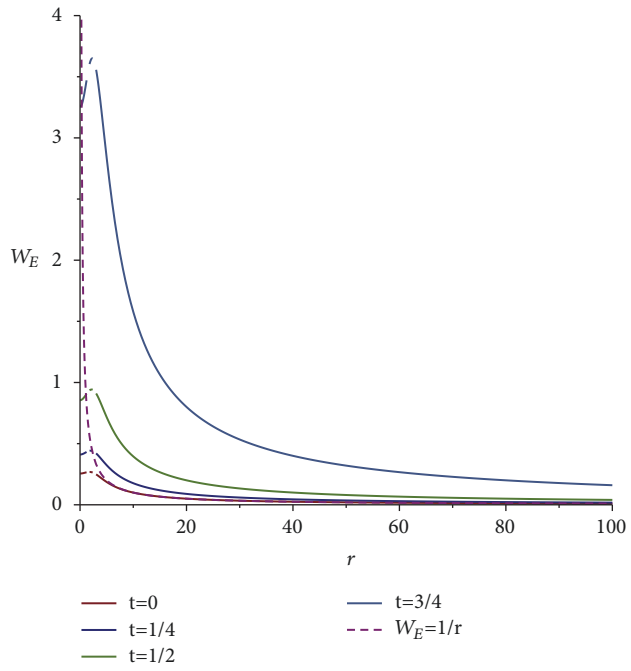

FIGURE 14: W_E for different times with $C_1 = C_2 = -1$ and $C_3 = C_4 = 1$.

physics. We plan to use the inhomogeneous Heisenberg chain model to discuss some physically relevant potential then.

ILL model is the continuum limitation of the discrete inhomogeneous Heisenberg chain, where the corresponding Heisenberg Hamiltonian (representing nearest neighbor interaction between S_i and S_{i+1}) is as follows:

$$H = -\Sigma_i q_i S_i S_{i+1}, \tag{103}$$

where S_i and S_{i+1} are on-site spins and q_i denotes the on-site ferromagnetic parameter which is the inhomogeneous physical interactions at the position i.

Equation (7) is a continuum model that can predicate any value of the site spin vector in a mathematical simulation way. Equation (7) plays a similar role as a Schrödinger equation for the Heisenberg model in quantum physics. As we can see in Section 1, the continuum limit of this system is also a nonlinear inhomogeneous Schrödinger equation (8) under the radial coordinates. For the discrete inhomogeneous Heisenberg chain, H or S_i has been used in the description of the magnetic properties and spin states of conjugated hydrocarbons and a large variety of metallic and organometallic compounds. What does the blowup solution (terminated in a finite time) represent in this discrete lattice system? In the continuum model ((7) or (8)), the blowup solution means that the gradient will be an infinite value, while the time is a finite time T. Accordingly, this finite time means that there are distortion and destruction in every position of i sites of a lattice. In this time T, there is a phase transition in the ferromagnetic solid.

Theorem 2 indicates that the phase transition (distortion and destruction) is possible under some special q_i. More clearly, if the exact quantitative scale of q is $r^{-n/2+2}$ as $r \longrightarrow +\infty$, this breaking down will happen in the ferromagnetic material. From a discrete point of view, i represents a correspondence of r by spatial position. The distribution $|i| \longleftrightarrow r$ means that the value of q_i is the value of $q(r)$. Hence, we expect that the phase transition in real ferromagnetic structure ($n = 3$) will begin in some blowup time T under the setting of $q_i \sim \sqrt{|i|}$ (as $|i| \longrightarrow +\infty$).

Multiple branches solution (see solution (62) in Section 3) allows a finite time blowup too. Accordingly, the discrete inhomogeneous Heisenberg chain of this system will generate a phase transition under some special setting of q_i. In particular, if $n = 3$ and $q_i \sim \sqrt{|i|}$ (as $|i| \longrightarrow +\infty$), the phase transition is a possible case in the multibranch elliptic case II according to Corollary 4. However, although (22) and (62) share a same breakdown in their discrete inhomogeneous Heisenberg chain system, the situation of multiple branches solution (62) is more complex than solution (22). For example, an energy gap can be found in the multibranch elliptic case II, while there is not any gap in solution (22). Why the energy gap will form in solution (62)? The most important reason is that there is a function arctanh in (58). If F touches the edges of the definition domain of arctanh, F jumps discontinuously from one value to another. In fact, if F touches the edges of the definition domain of arctanh, F will go to another track that belongs to the same multibranch. We can see that the difference between (22) and (62) is just a phase shift $C_2/(t-T)$ in the solution. From a point of the discrete inhomogeneous Heisenberg chain, the energy gap is inevitable due to the phase shift. This means that if we force the phase of the site spin vector to do a parallel movement, the jumping of the spin vector can be found in some location $|i|$ in any time before the blowup time. Furthermore, the scale of the jumping enlarges as the time goes on.

In the homogeneous Heisenberg chain ($q_i = 1$), all its lattice sites are equivalent. However, the self-consistent many-body ground states need not preserve all symmetries of the Hamiltonian in the inhomogeneous case. After the balance is broken, some singularity and jumping behaviors are possible according to the examples presented in the preceding sections. As we can see in these solutions, the Hamiltonian itself comprises inequivalent lattice sites that lead to the blowup and the energy gap. The inequivalent lattice sites are the case, for example, the Heisenberg chains with impurities or, more generally, the systems with different types of magnetic atoms. In the real problems, it is very common to find inhomogeneities rather than the homogeneous case. Actually, external nonuniform magnetic fields, anisotropic crystal fields, finite-size effects, boundary conditions, local impurities, lattice defects, and so forth can be induced for generalized inhomogeneities instances.

5. Conclusions

We investigated the evolution of the singular solution of n dimensional ILL on S^2. Two different ansatzes were applied in constructing the exact solutions in radially symmetric coordinates. Accordingly, two singular solutions were obtained ((22) and (62)). If one coefficient of (62) is set to 0, (62) degenerates into (22). All solutions show the same blowup

rate $(T-t)^{-1}$. However, (22) is a global solution on the entire spatial domain, whereas (62) contains some local and global subcases.

Energy density plays an important role in the energy analysis of these two solutions. The energy density decay rate (22) scales as $r^{n/2}$, which implies that the initial energy of this solution will be finite for $n > 3$. However, (62) is somewhat more complicated, with four subcases. If the coefficients of the solution (C_1, C_2, and C_3 in (62)) are suitably selected, the solution can be divided into four types: multibranch elliptic cases I and II and multibranch hyperbolic cases I and II. In contrast to (22), these subcases may lead to a new energy gap class of exact solutions.

One of these four cases is the global solution in the spatial domain. In this case, since the decay rate also scales as $r^{n/2}$, the initial energy is finite. The other three subcases can be local solutions, which means that the initial energy will be finite for any spatial dimension. All these multibranch cases lead to energy gaps in the energy density. The evolution of energy density for the cases was shown in Section 3, illustrating the decay property and monotonic increasing and decreasing behaviors. These evolutions were consistent with the theorem and corollary provided in Section 3. Thus, the multibranching of F for the solution plays a decisive role.

Integrability of the physical ILL has been investigated in [10]. The ILL discussed in this paper does not belong to the integrability system due to the inhomogeneous term. While many integrable spin systems are known, the integrability of IIL in the continuum limit has not been investigated. It will be of considerable interest to investigate the underlying singularity structures and energy gaps of such nonintegrable nonlinear evolution equations in detail. It would be also instructive to explore whether similar singular solutions can be obtained for LLE with Gilbert damping.

In conclusion, ILL and LLE display very interesting dynamic structures and further work is required to identify them.

Data Availability

The data used to support the findings of this study are available from the corresponding author upon request.

Conflicts of Interest

The author declares that he has no conflicts of interest.

Acknowledgments

This work is supported by NSFC (no. 11161057), National Science Foundation for Young Scientists of China (no. 11301014), TianYuan Special Fund of the National Natural Science Foundation of China (no. 11426068), Project for Young Creative Talents of Ordinary University of Guangdong Province (no. 2014KQNCX228), the PhD Start-up Fund of Natural Science Foundation of Guangdong Province (no. 2014A030310330), Research Award Fund for Outstanding Young Teachers in Guangdong Province (no. Yq20145084601), and Fund for Science and Technology of Guangzhou (no. 201607010352). The author is also grateful for the sponsorship from China Scholarship Council.

References

[1] L. D. Landau and E. M. Lifshitz, "On the theory of the dispersion of magnetic permeability in ferromagnetic bodies," in *Reproduced in Collected Papers of L. D. Landau*, Z. Sowjetunion, Ed., vol. 8, pp. 101–114, Pergamon, NY, USA, 1965.

[2] X. He, A. Qian, and W. Zou, "Existence and concentration of positive solutions for quasi-linear Schrodinger equations with critical growth," *Nonlinearity*, vol. 26, no. 12, pp. 3137–3168, 2013.

[3] Y. Sun, L. Liu, and Y. Wu, "The existence and uniqueness of positive monotone solutions for a class of nonlinear Schrödinger equations on infinite domains," *Journal of Computational and Applied Mathematics*, vol. 321, pp. 478–486, 2017.

[4] X. Zhang, L. Liu, Y. Wu, and Y. Cui, "Entire blow-up solutions for a quasilinear p-Laplacian Schrödinger equation with a non-square diffusion term," *Applied Mathematics Letters*, vol. 74, pp. 85–93, 2017.

[5] X.-N. Ma, P.-H. Wang, and W. Wei, "Constant mean curvature surfaces and mean curvature flow with non-zero Neumann boundary conditions on strictly convex domains," *Journal of Functional Analysis*, vol. 274, no. 1, pp. 252–277, 2018.

[6] F. Sun, L. Liu, and Y. Wu, "Infinitely many sign-changing solutions for a class of biharmonic equation with p-Laplacian and Neumann boundary condition," *Applied Mathematics Letters*, vol. 73, pp. 128–135, 2017.

[7] P. Wang and X. Wang, "The geometric properties of harmonic function on 2-dimensional Riemannian manifolds," *Nonlinear Analysis: Theory, Methods & Applications*, vol. 103, pp. 2–8, 2014.

[8] P. Wang and L. Zhao, "Some geometrical properties of convex level sets of minimal graph on 2-dimensional Riemannian manifolds," *Nonlinear Analysis: Theory, Methods & Applications*, vol. 130, pp. 1–17, 2016.

[9] R. Balakrishnan, "On the inhomogeneous Heisenberg chain," *Journal of Physics C: Solid State Physics*, vol. 15, no. 36, pp. L1305–L1308, 1982.

[10] M. Daniel, K. Porsezian, and M. Lakshmanan, "On the integrability of the inhomogeneous spherically symmetric Heisenberg ferromagnet in arbitrary dimensions," *Journal of Mathematical Physics*, vol. 35, no. 12, pp. 6498–6510, 1994.

[11] M. Han, L. Sheng, and X. Zhang, "Bifurcation theory for finitely smooth planar autonomous differential systems," *Journal of Differential Equations*, vol. 264, no. 5, pp. 3596–3618, 2018.

[12] F. Li and Q. Gao, "Blow-up of solution for a nonlinear Petrovsky type equation with memory," *Applied Mathematics and Computation*, vol. 274, pp. 383–392, 2016.

[13] F. Meng and J. Shao, "Some new Volterra-Fredholm type dynamic integral inequalities on time scales," *Applied Mathematics and Computation*, vol. 223, pp. 444–451, 2013.

[14] H. Tian and M. Han, "Bifurcation of periodic orbits by perturbing high-dimensional piecewise smooth integrable systems," *Journal of Differential Equations*, vol. 263, no. 11, pp. 7448–7474, 2017.

[15] L. Li, F. Meng, and Z. Zheng, "Oscillation results related to integral averaging technique for linear Hamiltonian systems," *Dynamic Systems and Applications*, vol. 18, no. 3-4, pp. 725–736, 2009.

[16] L. Li, F. Meng, and Z. Zheng, "Some new oscillation results for linear Hamiltonian systems," *Applied Mathematics and Computation*, vol. 208, no. 1, pp. 219–224, 2009.

[17] J. Liu and Z. Zhao, "Variational approach to second-order damped Hamiltonian systems with impulsive effects," *Journal of Nonlinear Sciences and Applications. JNSA*, vol. 9, no. 6, pp. 3459–3472, 2016.

[18] Z. Zheng, "Invariance of deficiency indices under perturbation for discrete Hamiltonian systems," *Journal of Difference Equations and Applications*, vol. 19, no. 8, pp. 1243–1250, 2013.

[19] P. Zhong, S. Wang, and S. Chen, "Some periodic and blow-up solutions for Landau-LIFshitz equation," *Modern Physics Letters A*, vol. 26, no. 32, pp. 2437–2452, 2011.

[20] P. Zhong, S. Wang, and M. Zeng, "Two blowup solutions for the inhomogeneous isotropic Landau-LIFshitz equation," *Journal of Mathematical Analysis and Applications*, vol. 409, no. 1, pp. 74–83, 2014.

[21] X.-G. Liu, "Concentration sets of the Landau-LIFshitz system and quasi-mean curvature flows," *Calculus of Variations and Partial Differential Equations*, vol. 27, no. 4, pp. 493–525, 2006.

[22] C. Wang, "On Landau-LIFshitz equation in dimensions at most four," *Indiana University Mathematics Journal*, vol. 55, no. 5, pp. 1615–1644, 2006.

[23] H. Huh, "Blow-up solutions of modified Schrödinger maps," *Communications in Partial Differential Equations*, vol. 33, no. 1-3, pp. 235–243, 2008.

[24] Q. Ding, "Explicit blow-up solutions to the Schrödinger R2 to the hyperbolic 2-space H2," *Journal of Mathematical Physics*, vol. 50, no. 10, 103507, 17 pages, 2009.

[25] F. Merle, P. Raphaël, and I. Rodnianski, "Blowup dynamics for smooth data equivariant solutions to the critical Schrödinger map problem," *Inventiones Mathematicae*, vol. 193, no. 2, pp. 249–365, 2013.

[26] J. B. van den Berg and J. F. Williams, "(In-)stability of singular equivariant solutions to the Landau-LIFshitz-Gilbert equation," *European Journal of Applied Mathematics*, vol. 24, no. 6, pp. 921–948, 2013.

[27] W. Ren and X.-P. Wang, "An iterative grid redistribution method for singular problems in multiple dimensions," *Journal of Computational Physics*, vol. 159, no. 2, pp. 246–273, 2000.

[28] X.-P. Wang and Carlos J., "A Gauss-Seidel projection method for micromagnetics simulations," *Journal of Computational Physics*, vol. 171, no. 1, pp. 357–372, 2001.

[29] S. Ding and C. Wang, "Finite time singularity of the Landau-LIFshitz-Gilbert equation," *International Mathematics Research Notices*, no. 4, Art. ID rnm012, 25 pages, 2007.

[30] S. Ding and J. Lin, "Partially regular solution to Landau-LIFshitz-Maxwell equations in two dimensions," *Journal of Mathematical Analysis and Applications*, vol. 351, no. 1, pp. 291–310, 2009.

[31] J. Lin and S. Ding, "Blow-up solutions to Landau-LIFshitz-Maxwell systems," *Mathematical Methods in the Applied Sciences*, vol. 34, no. 8, pp. 1006–1024, 2011.

[32] J. Lin and S. Ding, "Smooth solution to the one-dimensional inhomogeneous non-automorphic Landau-LIFshitz equation," *Proceedings of the Royal Society A Mathematical, Physical and Engineering Sciences*, vol. 462, no. 2072, pp. 2397–2413, 2006.

[33] Y. Li and Y. Wang, "Bubbling location for F-harmonic maps and inhomogeneous Landau-Lifshitz equations," *Commentarii Mathematici Helvetici*, vol. 81, no. 2, pp. 433–448, 2006.

[34] G. Yang, "The difference between Schrodinger equation derived from Schrödinger map and Landau-Lifshitz equation," *Physics Letters A*, vol. 376, no. 4, pp. 231–235, 2012.

[35] G. YANG, "Spherical cone symmetric families generated by Landau-Lifshitz equation and their evolution," *SCIENCE CHINA Mathematics*, vol. 41, no. 2, p. 181, 2011.

[36] G. Yang and B. Guo, "Some exact solutions to multidimensional Landau-LIFshitz equation with uprush external field and anisotropy field," *Nonlinear Analysis*, vol. 71, no. 9, pp. 3999–4006, 2009.

[37] B. Guo, Y. Han, and G. Yang, "Blow up problem for Landau-LIFshitz equations in two dimensions," *Communications in Nonlinear Science & Numerical Simulation*, vol. 5, no. 1, pp. 43-44, 2000.